$\alpha - \gamma$ transition in cerium: magnetic form factor and dynamic magnetic susceptibility in dynamical mean-field theory

B. Chakrabarti,[1] M. E. Pezzoli,[2,1] G. Sordi,[3,4] K. Haule,[1] and G. Kotliar[1]

[1]*Department of Physics & Astronomy, Rutgers University, Piscataway, NJ 08854-8019, USA*
[2]*Department of Physics and Astronomy, Stony Brook University, Stony Brook, New York 11794, USA*
[3]*SEPnet and Hubbard Theory Consortium, Department of Physics, Royal Holloway, University of London, Egham, Surrey TW20 0EX, United Kingdom*
[4]*Theory Group, Institut Laue Langevin, 6 rue Jules Horowitz, 38042 Grenoble Cedex, France*

(Dated: January 8, 2014)

The nature of the elemental cerium phases, undergoing an isostructural volume collapse transition, cannot be understood using conventional solid state concepts. Using the combination of density functional theory and dynamical mean-field theory, we study the magnetic properties of both the α and the γ phases. We compute the magnetic form factor, and show that it is very close to free ion behavior in both the local moment γ phase as well as the more itinerant α phase, in agreement with neutron scattering experiments. In sharp contrast, the dynamic local magnetic susceptibility of the two phases is strikingly different. In the γ phase, the sharp low energy peak due to local moment formation and consequently low Kondo temperature dominates the spectra. In the α phase two broad peaks can be identified, the first is due to Kondo screening, and the second is due to Hund's coupling. This shows that hybridization plays a central role in the $\alpha - \gamma$ transition in cerium, and that from the point of view of magnetic properties, the $4f$ electrons are strongly correlated in both phases.

PACS numbers: 71.27.+a, 71.30.+h

arXiv:1401.1245v1 [cond-mat.str-el] 7 Jan 2014

The physical mechanism driving the α-γ phase transition has puzzled physicists for many years [1]. Similar to other elements, the temperature versus pressure phase diagram of cerium shows multiple structural transitions, where the symmetry of the structure changes across the phase transition. The α-γ transition is exceptional because it is isostructural, i.e. the atoms retain their ordering in an fcc structure while the volume collapses by 15% from γ to α phase upon increasing pressure. Moreover, the $\alpha - \gamma$ transition is accompanied by a dramatic change in the magnetic susceptibility: the α phase shows Pauli-like susceptibility, while the γ phase has Curie-like susceptibility. Therefore, most of the theoretical work has focused on the hypothesis that electronic effects are responsible for the transition.

Numerous theoretical models were proposed to explain the isostructural transition in Ce. For example, in the promotional model [2], the $4f$ electrons are localized in the γ phase, and are promoted to the *spd* conduction band in the α phase. However photoemission spectroscopy shows little change in the number of the conduction electrons at the transition. Johansson proposed [3] that the $\alpha - \gamma$ transition is an example of a Mott transition. Here the $4f$ electrons undergo a Mott transition, from a non-bonding localized state in the γ phase to a narrow $4f$ band in the α phase, which participates in bonding. The *spd* electrons remain bystanders during the transition. Upon increasing pressure, a $4f$ localization-delocalization transition occurs with a subsequent loss of moment and decrease of volume. In this model, the $4f$ electron number remains almost unchanged with pressure, so this feature is consistent with photoemission results. A different scenario was proposed by Lavagna et al. [4] and Allen [5], dubbed the Kondo volume collapse theory. Here the *spd* electrons are not bystanders as in the Mott scenario. Instead the transition is connected to the change in the effective hybridization (and thus the Kondo scale) of the *spd* electrons with the $4f$ electrons and so there is a decrease in volume due to the increase of the Kondo temperature T_K.

Dynamical mean-field theory (DMFT) [6] is a modern tool to understand the physics of strong electron correlations. The combination of density functional theory (DFT) and DMFT [7, 8] (DFT+DMFT) allows one to consider structural effects, electronic effects and the physics of strong correlations from first-principles. It brings the physics of f-electron delocalization and f-spd hybridization into a unified framework. As a result of many studies over several years, different aspects of the $\alpha - \gamma$ transition have been considered, including changes in the density of states [9–11], in the optical conductivity [12], and in the thermodynamic properties [13, 14].

From the theoretical point of view, the magnetic properties of the volume collapse transition have not been adequately addressed so far. The static local and the uniform magnetic susceptibility was computed in Ref. 15 using charge non-self-consistent DFT+DMFT, but the local susceptibility turned out to be similar in both phases and the magnetic susceptibility was underestimated due to negligence of spin orbit coupling, which was shown to be crucial for proper description of α-γ transition in cerium [14]. As shown in this letter, the orbital moment dominates the magnetic moment in cerium, and is quenched when spin-orbit coupling is neglected. Re-

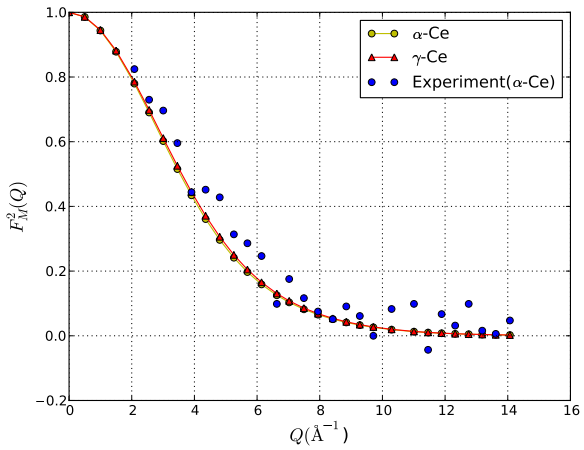

FIG. 1: Momentum transfer dependence of the normalised magnetic form factor $F_M^2(Q)$ of α-Ce and γ-Ce. Blue circles show experimental data taken from Ref. 16.

cently, compelling neutron scattering experiments [16] were performed, which call for theoretical analysis. Here we shall revisit the $\alpha-\gamma$ transition from the point of view of magnetic properties by computing the magnetic form factor $F_M(q)$, the local dynamic susceptibility $\chi(\omega)$ and the magnetic spectral response $S(q,\omega)$. We shall show that the magnetic form factor shows free ion behavior in both phases, indicating that from the point of view of magnetic properties, the $4f$ electrons are strongly correlated both in the α and γ phases. The dynamic magnetic susceptibility of the two phases is very different. It shows a sharp low energy peak at the characteristic energy, which scales with the coherence temperature of each phase. Since the coherence scale is directly connected with the strength of hybridization, this suggests that the hybridization plays a central role in the $\alpha-\gamma$ transition in cerium.

Model and method.– In this Letter, we have performed DMFT+DFT calculations in a charge self-consistent implementation [8]. For the Kohn-Sham potential, we used the GGA functional as implemented in Wien2k package [17], and continuous-time quantum Monte Carlo (CTQMC) method to solve the auxiliary impurity problem [18]. We used Hubbard repulsion $U = 6.0$eV, Hund's coupling $J = 0.7$eV, and temperature $T = 116K$. The lattice constants of the fcc unit cell are $a \approx 4.82\mathring{A}$ and $a \approx 5.16\mathring{A}$ for the α and γ phases respectively.

Magnetic form factor.– The magnetic form factor $F_M(q)$ is the Fourier transform of the spatial distribution of the electronic magnetic moment, here mostly contributed by $4f$ electrons. Thus it is an ideal observable for determining the nature of the $4f$ electrons. In particular, the magnetic form factor can determine whether $4f$ electrons are localised or itinerant, as suggested in

	α-Ce	γ-Ce
μ_s	-2.3079×10^{-3}	-0.03468
μ_L	9.3668×10^{-3}	0.13841
C_2	1.327	1.334

TABLE I: Values of the orbital (μ_L) and spin μ_S magnetic moment as obtained in our DFT+DMFT calculations under a magnetic field of 10T. The coefficient $C_2 = \mu_L/(\mu_L + \mu_S)$ determines the shape of the form factor in the dipole approximation and has similar value in both phases.

Ref. 19. The idea is the following: band formation results in the quenching of the $4f$ magnetic moment, especially the orbital component relative to the spin component. Thus, if the volume collapse is due to a localisation-to-delocalisation transition, there should be a dramatic change between the shape of the magnetic form factor between the α and γ phases. For γ cerium, the measured magnetic form factor has free ion behavior, which is in good agreement with the computed ionic Ce^{3+} magnetic form factor [20]. On the other hand, for the α cerium, electronic structure calculations predict metal-like behavior for the magnetic form factor [19]. However, these calculations are in striking contrast with recent high-energy neutron inelastic measurements by Murani et al. [16], which show free ion behaviour for the magnetic form factor of α cerium as well.

Following the formalism described in Ref. 21, we compute the magnetic form factor within the DFT+DMFT framework. Figure 1 shows the magnetic form factor squared $F_M^2(q)$ in presence of an external magnetic field for both α and γ cerium. The curves are close to each other and display free ion behavior, typical of a correlated state. This is a consequence of the electron-electron Coulomb repulsion, and cannot be captured solely by electronic band structure effects. Our results are in good agreement with the measured magnetic form factor of α cerium of Ref. [16], and show that electronic structure calculations, when combined with the dynamical mean-field theory, have the predictive power to capture the magnetic response of the $4f$ electrons, and therefore to reconcile theory and neutron scattering experiment.

To gain a deeper understanding of these results, we resort to dipole approximation, $F_M = \mu(\langle j_0\rangle + C_2\langle j_2\rangle)$, where $\langle j_k\rangle = \int dr\ u(r)J_k(qr)$ is the spatial average of the spherical Bessel function $J_k(qr)$ over the atomic cerium wave function $u(r)$, $\mu = \mu_S + \mu_L$ is the total (spin plus orbital) magnetic moment, and $C_2 = \mu_L/(\mu_S + \mu_L)$. As shown in Table I, μ_L and μ_S have opposite sign because of third atomic Hund's rule (that is because of spin-orbit coupling and $n_f < 1$), and $\mu_L > \mu_S$, thus $C_2 > 0$. The coefficient C_2 determines the shape of $F_M(q)$ and remains basically unchanged across the $\alpha - \gamma$ transition. It is close to the one expected for a free Ce^{3+} ion, implying that there is a localised $4f$ electronic density for both α

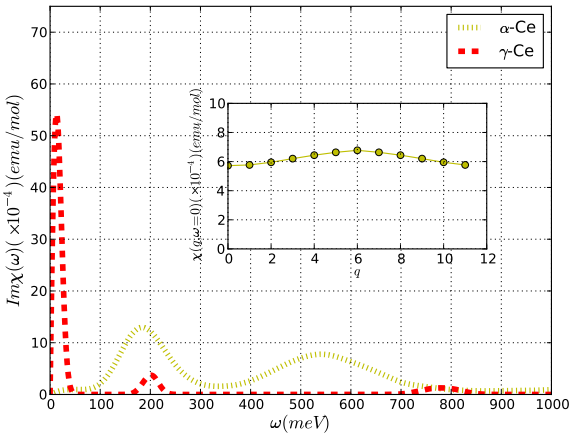

FIG. 2: Imaginary part of the local dynamic magnetic susceptibility, Im$\chi(\omega)$, for α and γ cerium (yellow dotted and red dashed lines respectively). The inset shows the static susceptibility $\chi(q, \omega = 0)$ of α cerium as a function of q in the first Brillouin zone. Note that the q goes from the points (0,0,0) to (1,1,-1) in 12 uniform steps.

and γ cerium.

Local dynamic magnetic susceptibility.– The magnetic form factor indicates that both α and γ phase are strongly correlated phases, which is compatible with both Mott and Kondo volume collapse scenarios, but eliminates the promotional model. In the Mott scenario, the two phases are correlated because they lie on slightly opposite sides of the delocalisation-localisation transition, while in the Kondo volume collapse picture, the two phases are correlated because the $4f$ electron moment remains stable across the transition. However, the Kondo volume collapse scenario differs from the Mott scenario because it does not consider the *spd* electrons to be mere bystanders, but emphasizes their role in the screening of the local magnetic moments, via the Kondo effect. Therefore, the dynamic magnetic susceptibility, which measures the spatial and temporal distribution of the magnetic fluctuations, can indicate whether the hybridization plays a key role at the transition.

In our calculations, we used the CTQMC impurity solver to obtain the local dynamic susceptibility $\chi(i\omega_n)$ of α and γ cerium as a function of Matsubara frequencies. We then analytically continued the data using maximum entropy method to obtain Im $\chi(\omega)$ along the real frequency axis. In Figure 2 we show Im $\chi(\omega)$ for both phases. At small frequencies, Im $\chi(\omega)$ for γ cerium shows a narrow and intense magnetic peak centered at approximately 10 meV. This feature has to be expected from the local moment character of electrons in γ cerium. The position of this peak gives a measure of the Kondo temperature T_K. For α cerium, this peak shifts to higher frequency, around 180 meV. Thus, in going from γ to α phase, there is a shift of magnetic intensity from low to high energy, signalling a change (precisely, an increase) in T_K. This is one of the central results of our work. We emphasize that, at large frequencies, the overall intensity of Im $\chi(\omega)$ in the α phase is larger than in the γ phase, reflecting the increased hybridization of electrons in the former phase.

In order to ascertain the nature of the different peaks in the dynamic susceptibility of α cerium, we performed simulations of the α phase with different values of spin-orbit coupling (not shown). Upon increasing spin-orbit coupling, the peak at low frequency (≈ 180 meV) moves towards $\omega = 0$. This is a feature of the fact that by increasing the spin-orbit coupling, the effective Kondo temperature of the system is reduced. Hence this peak is a feature of the Kondo coherence energy of the system. This trend has to be expected because of the hybridisation between the conduction electrons and the f electrons. By increasing the spin orbit coupling, the energy splitting between the 5/2 and 7/2 states increases, therefore fluctuations are hampered and 7/2 states are less occupied. It follows that the hybridisation with conduction electrons decreases as well. The importance of the spin-orbit coupling has also been emphasized in the cerium compounds $CeIn_{3-x}Sn_x$ and $CePd_3$ [22–24].

The second peak (≈ 600 meV) however does not show sensitivity to the spin-orbit coupling. To further ascertain the origin of the second peak, we performed simulations with altered values of Hunds Coupling J (not shown). The second peak is always roughly centred at $\omega = J$ indicating that it represents an excitation of the the f-electrons in the (non-zero) doubly occupied sector of f-electron occupancy.

Notice that to crosscheck the validity of our analytic continuation procedure, we benchmarked our results against a well-known sum rule for Im$\chi(\omega)$. It is known that $\frac{1}{\pi}\int_{-\infty}^{\infty} n(\omega) Im\chi(\omega) d\omega = \langle \mu_z^2 \rangle$ where $n(\omega)$ is the Bose distribution function and μ_z is the magnetic moment along the z axis, which can be independently extracted in our simulation without need of analytic continuation. A good quantitative agreement is obtained in both phases.

In addition, we have verified that the local dynamical susceptibility $\chi(\omega)$ is a good representative of the behavior of the susceptibility $\chi(q, \omega)$ within the first Brillouin zone. This is important, because it verifies the so-called "single-ion form factor dependence" often used to analize experimental data [16], where the dynamical structure $S(q, \omega)$ is factorized into momentum dependent form factor $F_M(q)^2$, and energy dependent structure factor $S(\omega) = \frac{1}{2}\frac{1}{1-e^{-\beta\hbar\omega}}Im\chi(\omega)$, i.e, $S(q, \omega) = F_M(q)^2 S(\omega)$. To verify the quality of this approximation, we have computed the static susceptibility $\chi(q, \omega = 0)$ of α cerium within the first Brillouin zone using a two particle vertex

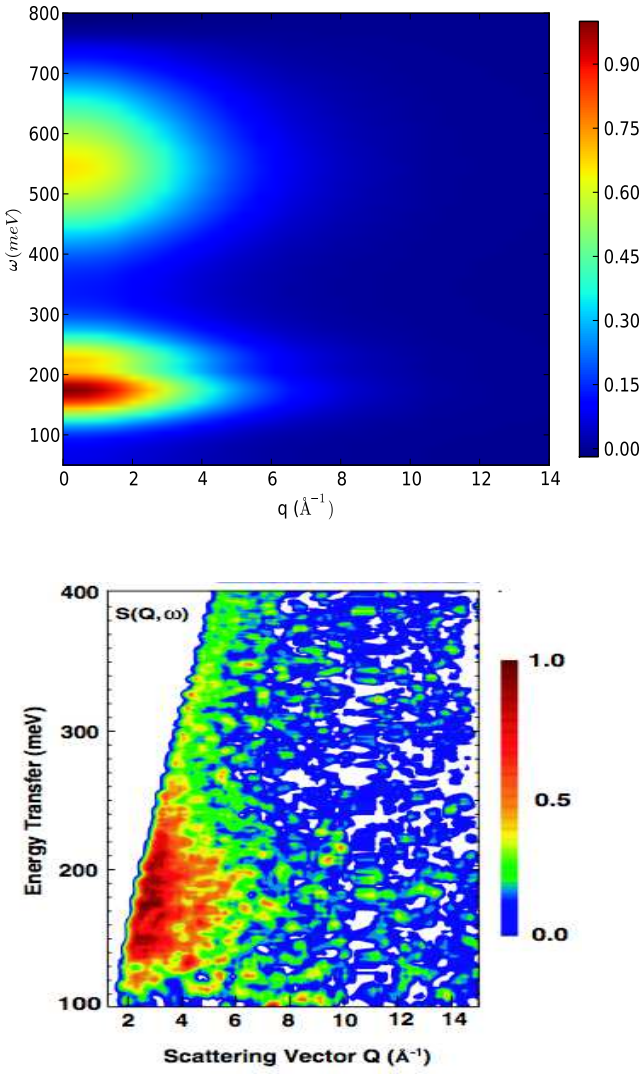

FIG. 3: Difference of $S(q,\omega)$ between α and γ phase : Top panel shows DFT+DMFT results. Lower panel shows high energy neutron inelastic measurements, taken from Ref [16].

method, developed in Ref. 25. We calculate $\chi(q)$ using the Bethe-Salpeter equation $\chi(q) = (\chi_0^{-1}(q) - \Gamma)^{-1}$, where Γ is the two particle irreducible vertex, which we sample within DMFT, and χ_0 is the RPA susceptibility, which we compute using the full k-dependent LDA+DMFT green's function. Note that within DMFT, the two particle irreducible vertex Γ is local. The inset of Figure 2 shows $\chi(q, \omega = 0)$. We can see that there is no significant variation in the static susceptibility within the first Brillouin zone, which validates the "single-ion form factor formula".

Magnetic spectral response.– We then use this formula to compute frequency dependent $S(q,\omega)$ of both phases. Figure 3 shows the difference between the α and γ magnetic spectral response $(S_\alpha(q,\omega) - S_\gamma(q,\omega))$. In the lower panel we show the experimental spectrum [16]. There is a good agreement between the two, particularly in the position of the broad peak assigned to the Kondo screening in the α-phase. Note that the spectrum displayed in Fig. 3 becomes negative in the low energy region where γ-Ce susceptibility has sharp peak due to local moment character (see Fig. 2). This region has been left out of theoretical (as well as experimental) plot so as to enable better visualization of the other features.

In summary, we showed theoretically that the neutron magnetic form factor $F_M(q)$ has a free ion behaviour in both phases, indicating that the $4f$ electrons remain strongly correlated across the α-γ transition. On the other hand, the local dynamical susceptibility $\chi(\omega)$ and the magnetic spectrum $S(q,\omega)$ show dramatic changes across the transition, with an energy shift from lower to higher frequencies, a direct consequence of the increase of the Kondo temperature T_K in the α cerium. Therefore, our data shows that the physics of the volume collapse α-γ transition in cerium is controlled by the hybridization between the localised $4f$ and the *spd* electrons and also establishes the importance of using different probes and observables to understand different aspects of the volume collapse transition in cerium.

Acknowledgment.– M.E.P. and G.S. thank A. Murani for enlightening discussions. This work was partially supported by NSF DMR-0746395 (K.H.) and and DE-FG02-99ER45761(G.K)

[1] D. Koskenmaki and J. K.A. Gschneidner, *Cerium, Handbook on the Physics and Chemistry of Rare Earths, Vol 1, KA. Gschneidner, Jr. and L. Eyring, Ed.* (Elsevier, North-Holland, Amsterdam, 1978).
[2] B. Coqblin and A. Blandin, Advan. Phys. p. 281 (1968).
[3] B. Johansson, Philosophical Magazine. **30**, 469 (1974).
[4] M. Lavagna, C. Lacroix, and M. Cyrot, Physics Letters A **90**, 210 (1982), ISSN 0375-9601, URL http://www.sciencedirect.com/science/article/B6TVM-46SNMSW-
[5] J. W. Allen and R. M. Martin, Phys. Rev. Lett. **49**, 1106 (1982), URL http://link.aps.org/doi/10.1103/PhysRevLett.49.1106.
[6] A. Georges, G. Kotliar, W. Krauth, and M. J. Rozenberg, Rev. Mod. Phys. **68**, 13 (1996), URL http://link.aps.org/doi/10.1103/RevModPhys.68.13.
[7] G. Kotliar, S. Y. Savrasov, K. Haule, V. S. Oudovenko, O. Parcollet, and C. A. Marianetti, Rev. Mod. Phys. **78**, 865 (2006), URL http://link.aps.org/doi/10.1103/RevModPhys.78.865.
[8] K. Haule, C.-H. Yee, and K. Kim, Phys. Rev. B **81**, 195107 (2010), URL http://link.aps.org/doi/10.1103/PhysRevB.81.195107.
[9] M. B. Zölfl, I. A. Nekrasov, T. Pruschke, V. I. Anisimov, and J. Keller, Phys. Rev. Lett. **87**, 276403 (2001), URL http://link.aps.org/doi/10.1103/PhysRevLett.87.276403.

[10] K. Held, A. K. McMahan, and R. T. Scalettar, Phys. Rev. Lett. **87**, 276404 (2001), URL http://link.aps.org/doi/10.1103/PhysRevLett.87.276404.
[11] A. K. McMahan, K. Held, and R. T. Scalettar, Phys. Rev. B **67**, 075108 (2003), URL http://link.aps.org/doi/10.1103/PhysRevB.67.075108.
[12] K. Haule, V. Oudovenko, S. Y. Savrasov, and G. Kotliar, Phys. Rev. Lett. **94**, 036401 (2005), URL http://link.aps.org/doi/10.1103/PhysRevLett.94.036401.
[13] B. Amadon, S. Biermann, A. Georges, and F. Aryasetiawan, Phys. Rev. Lett. **96**, 066402 (2006), URL http://link.aps.org/doi/10.1103/PhysRevLett.96.066402.
[14] N. Lanatà, Y.-X. Yao, C.-Z. Wang, K.-M. Ho, J. Schmalian, K. Haule, and G. Kotliar, Phys. Rev. Lett. **111**, 196801 (2013), URL http://link.aps.org/doi/10.1103/PhysRevLett.111.196801.
[15] S. V. Streltsov, E. Gull, A. O. Shorikov, M. Troyer, V. I. Anisimov, and P. Werner, Phys. Rev. B **85**, 195109 (2012), URL http://link.aps.org/doi/10.1103/PhysRevB.85.195109.
[16] A. P. Murani, S. J. Levett, and J. W. Taylor, Phys. Rev. Lett. **95**, 256403 (2005).
[17] P. Blaha, K. Schwarz, G. K. H. Madsen, D. Kvasnicka, and J. Luitz, *WIEN2K, An Augmented Plane Wave + Local Orbitals Program for Calculating Crystal Properties* (Karlheinz Schwarz, Techn. Universität Wien, Austria, 2001).
[18] K. Haule, Phys. Rev. B **75**, 155113 (2007), URL http://link.aps.org/doi/10.1103/PhysRevB.75.155113.
[19] A. Hjelm, J. Trygg, O. Eriksson, B. Johansson, and J. Wills, Phys. Rev. B **50**, 4332 (1994), URL http://link.aps.org/doi/10.1103/PhysRevB.50.4332.
[20] C. Stassis, C.-K. Loong, G. Kline, O. McMasters, and K. Gschneider, J. Appl. Phys. **49**, 2113 (1978).
[21] M. E. Pezzoli, K. Haule, and G. Kotliar, Phys. Rev. Lett. **106**, 016403 (2011), URL http://link.aps.org/doi/10.1103/PhysRevLett.106.016403.
[22] A. P. Murani, A. D. Taylor, R. Osborn, and Z. A. Bowden, Phys. Rev. B **48**, 10606 (1993), URL http://link.aps.org/doi/10.1103/PhysRevB.48.10606.
[23] A. P. Murani, R. Raphel, Z. A. Bowden, and R. S. Eccleston, Phys. Rev. B **53**, 8188 (1996), URL http://link.aps.org/doi/10.1103/PhysRevB.53.8188.
[24] N. E. Bickers, D. L. Cox, and J. W. Wilkins, Phys. Rev. B **36**, 2036 (1987), URL http://link.aps.org/doi/10.1103/PhysRevB.36.2036.
[25] H. Park, K. Haule, and G. Kotliar, Phys. Rev. Lett. **107**, 137007 (2011), URL http://link.aps.org/doi/10.1103/PhysRevLett.107.137007.